

MDPI

Article

Identification of Five Robust Novel Ene-Reductases from Thermophilic Fungi

Pedro H. Damada 1,2 and Marco W. Fraaije 1,* D

- Molecular Enzymology Group, University of Groningen, Nijenborgh 3, 9747 AG Groningen, The Netherlands; pedrodamada@usp.br
- Laboratório de Química Orgânica e Biocatálise, Instituto de Química de São Carlos, Universidade de São Paulo, Av. João Dagnone 1100, "Ed. Prof. Wagner Douglas Franco", Santa Angelina, São Carlos 13563-120, SP, Brazil
- * Correspondence: m.w.fraaije@rug.nl

Abstract: Ene-reductases (ERs) are enzymes known for catalyzing the asymmetric hydrogenation of activated alkenes. Among these, old yellow enzyme (OYE) ERs have been the most extensively studied for biocatalytic applications due to their dependence on NADH or NADPH as electron donors. These flavin-containing enzymes are highly enantio- and stereoselective, making them attractive biocatalysts for industrial use. To discover novel thermostable OYE-type ERs, we explored genomes of thermophilic fungi. Five genes encoding ERs were selected and expressed in Escherichia coli, namely AtOYE (from Aspergillus thermomutatus), CtOYE (from Chaetomium thermophilum), LtOYE (from Lachancea thermotolerans), OpOYE (from Ogatae polymorpha), and TtOYE (from Thermothielavioides terrestris). Each enzyme was purified as a soluble FMN-containing protein, allowing detailed characterization. All ERs exhibited a preference for NADPH, with AtOYE showing the broadest substrate range. Moreover, all the enzymes showed activity toward maleimide and p-benzoquinone, with TtOYE presenting the highest catalytic efficiency. The optimal pH for enzyme activity was between 6 and 7 and the enzymes displayed notable solvent tolerance and thermostability, with CtOYE and OpOYE showing the highest stability ($T_m > 60\,^{\circ}$ C). Additionally, all enzymes converted R-carvone into (R,R)-dihydrocarvone. In summary, this study contributes to expanding the toolbox of robust ERs.

Keywords: biocatalysis; Ene-reductases (ERs); enzyme; old yellow enzyme; flavin



Citation: Damada, P.H.; Fraaije, M.W. Identification of Five Robust Novel Ene-Reductases from Thermophilic Fungi. *Catalysts* **2024**, *14*, 764. https://doi.org/10.3390/catal14110764

Academic Editors: Chia-Hung Kuo, Chwen-Jen Shieh and Yung-Chuan Liu

Received: 8 October 2024 Revised: 23 October 2024 Accepted: 28 October 2024 Published: 29 October 2024



Copyright: © 2024 by the authors. Licensee MDPI, Basel, Switzerland. This article is an open access article distributed under the terms and conditions of the Creative Commons Attribution (CC BY) license (https://creativecommons.org/licenses/by/4.0/).

1. Introduction

Ene-reductases (ERs) encompass a diverse group of enzymes able to catalyze the asymmetric *trans*-hydrogenation of activated alkenes, rendering them highly attractive biocatalysts [1,2]. These redox enzymes are divided in different ER families according to characteristics, such as cofactor dependency, structural attributes, and substrate scope [3,4]. The most well studied ER is the so-called old yellow enzyme (OYE) from the yeast *Saccharomyces carlsbergensi* [5], which was already isolated in 1932. This prototype ER is currently referred to as OYE1, and the term 'old yellow enzyme' is used to indicate a particular and widespread family of FMN-containing ERs. For a few decades, OYE-type ERs have been recognized as valuable biocatalysts and are used in industrial applications [6].

Currently, OYE-type ERs are classified into different classes, based on sequence similarity. Initially, three classes were identified [7]. However, with the discovery of novel ERs, the number of classes has expanded to seven. Each class has specific characteristics. Class I ERs are predominantly represented by bacteria and plants and exclusively comprise 'classical' ene-reductases. Class II ERs encompass 'classical' enzymes isolated from fungi and include the well-known OYE1. The enzymes from these two classes have been found to be monomeric or dimeric. Conversely, Class III harbors larger oligomeric enzymes, exemplified by the bacterial YqjM [8], a homotetrameric ER. The discovery of this enzyme

contributed to the distinction between 'classical' and 'thermophilic-like' ERs with the latter being distinct in active site and structure when compared with the 'classical' ERs. Most of the enzymes within Class III were classified as 'thermophilic-like', with representatives from bacteria and algae, having monomeric, dimeric, or higher oligomeric forms. Information on ERs from the remaining four classes is scarce, and further research is needed to gain a comprehensive understanding of their properties and functions [9].

An interesting characteristic of OYE-type ERs is the high chemo- and stereoselectivity achieved after the reduction of alkenes, enabling the production of chiral products. This feature is highly relevant for their applications in synthetic chemistry as biocatalysts [10-12]. Different from the use of chemical catalysts, the ER-catalyzed reactions can be performed under mild conditions. This is another aspect of considerable advantage contributing to the sustainability of ER-based catalytic processes [13]. The high stereoselectivity of ERs can be better understood by examining the reaction mechanism (Figure 1). OYEs harbor a tightly bound FMN cofactor that is crucial for the reduction of the accepted substrate. For being able to perform a reduction, the flavin first is reduced by a hydride transfer from a nicotinamide adenine dinucleotide cofactor (NADH or NADPH depending on the ER). In the subsequent reaction, the reduced ER transfers the hydride from the reduced FMN to the activated alkene. The substrate carbon which receives this hydride is designated as β, while the carbon bound to the electron-withdrawing group is designated as the α carbon. Upon hydride transfer to the substrate, the α carbon is protonated, typically assisted by a conserved tyrosine residue located in the active site of the enzyme. This protonation step completes the *trans*-reduction process [14–16].

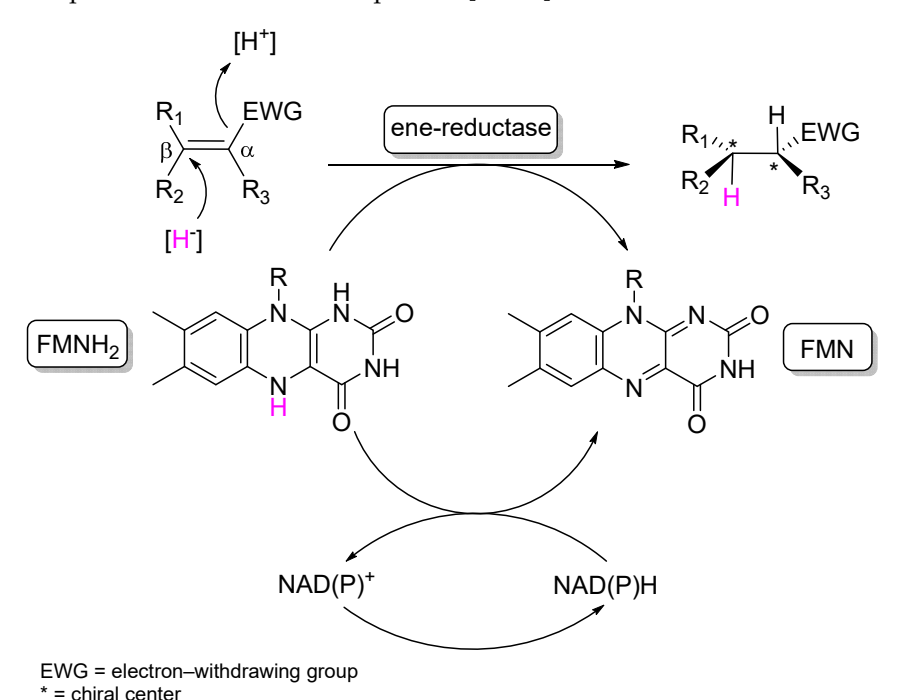


Figure 1. Asymmetric reduction of activated alkenes by ene-reductases (ERs).

The search for new ERs continues to be of great interest, particularly those exhibiting enhanced thermostability, as numerous industrial processes are conducted at elevated temperatures and/or challenging conditions. Consequently, thermophilic microorganisms are often screened for the presence of ERs. However, most of such enzyme discovery efforts have focused on meso- and thermophilic bacteria, while thermophilic fungi have hardly been explored for this [17–20]. This may be partly because the expression of fungal enzymes in regular bacterial expression hosts, such as *Escherichia coli*, is often found to be problematic. This is often due to post-translational modifications that are not feasible in bacteria, such as glycosylation.

Catalysts **2024**, 14, 764 3 of 16

In this study, we explored fungi that can grow at temperatures of 50–55 °C [21]. At such high temperatures, it can be expected that the enzymes produced and utilized by these fungi are relatively thermostable compared to ERs from microbes that thrive at moderate temperatures. Specifically, we focused on the predicted proteomes of the following thermophilic fungi for the discovery of OYE-type ERs: *Aspergillus thermomutatus* [22,23], *Chaetomium thermophilium* [24], *Thermothielavioides terrestris* [25], *Lachancea thermotolerans* [26], and *Ogataea polymorpha* [27]. Here, we report on the expression and biocatalytic properties of the five respective OYEs.

2. Results and Discussion

2.1. Identification and Sequence Analyses of New Putative ERs

Genes encoding for putative ERs from thermotolerant fungi were identified by using the BLASTp tool (NCBI, Bethesda, MD, USA). The sequence of the prototype ER, OYE1, was used as a query to search for homologs in fungal genomes. From the obtained hits with high sequence identities, sequences originating from thermotolerant fungi were selected. This resulted in the selection of five putative ERs, namely AtOYE (putative ER from Aspergillus thermomutatus), CtOYE (putative ER from Chaetomium thermophilium), LtOYE (putative ER from Lachancea thermotolerans), OpOYE (putative ER from Ogatae polymorpha), and TtOYE (putative ER from Thermothielavioides terrestris). The highest identity with OYE1 was observed for LtOYE (sequence identity of 73%), while the others putative ERs displayed only 41-43% sequence identity. The five selected protein sequences were aligned with known ERs to create a phylogenetic tree (Figure 2). In line with the most recent classification of OYE-type ERs, all fungal proteins selected for this study were found to be Class II ERs. This group of ERs is known to be populated by fungal ERs, including OYE1. It is important to note that so far, known Class II ERs originated from mesophilic microorganisms. Here, we explored Class II ERs derived from thermophilic fungi for which it is expected that they are relatively stable enzymes.

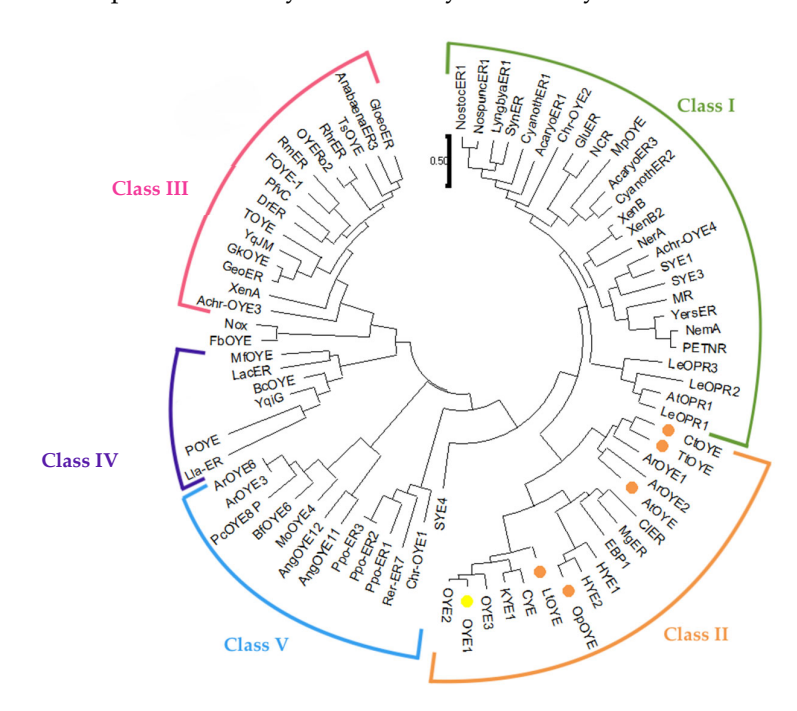


Figure 2. Phylogenic tree constructed using the protein sequences selected for this study and ERs described in the literature [7]. The analysis involved 79 protein sequences. The enzymes of this study (AtOYE, CtOYE, LtOYE, OpOYE, and TtOYE) are tagged by small orange dots. OYE1 is tagged with a small yellow dot.

OYE-type ERs have been subject of many biochemical studies, resulting in the identification of specific sequence patterns. Such sequence features can help in predicting or

Catalysts 2024, 14, 764 4 of 16

explaining enzyme properties. We carefully analyzed the five newly identified ERs by comparing their sequences with the prototype ER, OYE1 (Figure 3). Oberdorfer et al. [28] noted that monomeric and dimeric ERs can be differentiated at the sequence level; monomeric ERs have a conserved pattern in the region near loop $\beta 2$ (G-[FYW]-X(3)-P-G-[ILV]-[FHYW]) and another in the region of loop $\beta 1$ (P-[LM]-T-R-X-R). CtOYE, LtOYE, and TtOYE comply with these two sequence motifs, which suggests that these fungal ERs are monomeric (Figure 3). In the other two ERs, AtOYE and OpOYE, some variations were observed (Figure 3, red letters), which may hint to aberrant oligomeric compositions.

```
Atoye
CtOYE
            ------MTEVK 5
Lt0YE
0p0YE
           MPAIENHVSGNVSTRAARIPSADMSALGDLNSRTKTTESATSASAHLPAQHIAVGIARVI 60
Tt0YE
0YE1
           -----MSKLFSPIOVG-RMOLGHRLAMAPMTRFRADD-DHVPL-PMVKDHYEORAAV 49
AtOYE
            ---MSPSNNTRLFEPLQLG-TVTLSHRIAMAPLTRFRALD-SHVPQLPLVAEYYTQRASI 55
CtOYE
           DLKPIALQDTKLFEPIQIG-DTTVEHRAVMCPLTRMRAHHPGNVPNKDWALEYYDQRSKA
           MSKTPTLANTNLFKPIKVG-KVELKNRLVFA<mark>PTTRYR</mark>ASK-DFVPT-DSMLKYYEQRAEN 117
0p0YE
           ---MTITAESRLFOPLKLTPKITLAHRVAMA<mark>PLTRYR</mark>ASD-EHVPLVPLVANYYGORASV
DFKPQALGDTNLFKPIKIG-NNELLHRAVIP<mark>PLTRMR</mark>ALHPGNIPNRDWAVEYYTQRAQR
Tt0YE
0YE1
                                   : :* .: * ** ** .
           PGTLLITEATLVSPRAGSYPNVPGIWSEAOIAOWROVTDAVHAKGSYIYMOLWGLGRVAN 109
A±0YE
           PGTLLITEGTFIAOHAGGLPNIPGIWNEDOIKAWKVVTDAVHAKGSFIFCOLWALGRAAN
CtOYE
           PGTMIITEGTFPSPQCGGYDNAPGIWSKEQIEQWKKIFAKIHENKSFAWVQLWVLGRQAF
           NGGLLVTEATYPDYSFGLYPDTPMIKTPAQVAGWKKVIEAVHNKGSFVSIQLWHLGRTAS 177
0p0YE
T±0YE
           PGTLLVTEATFVAPAAGGYANVPGIYNAAQVAAWRRVTDAVHARGSYIFLOLWSLGRTAH 116
           PGTMIITEGAFISPQAGGYDNAPGVWSEEQMVEWTKIFNAIHEKKSFVWVQLWVLGWAAF
                              : * : . *: * : :* . *:
A+0YF
           PETI KKEGGEDI VSSSDVPT-D-----FTAPAPRAI TEFETHAETADYAOAARNATA 160
           PKVAEA-EGFKVKSSSAVPI-E------EGGVVPEEMTVEEIKEMVKAYANAARNAIK 165
CtOYE
Lt0YE
           PDTLKR-DGLRYDSASDEVYMDDASEKKAIECDNROHGITKEEIKOYVKDYVOAAKNSID 183
           AEFNKS-KGLPLVGASPI-YMDEDSEKAAKEAGNELRELTIPEIEAIVKEFAAAAKRAIH 235
0p0YE
T+0YF
           PDELAK-DGFRLKAPSALPM-E-----EGAPVPEPMTVEEIOORVRDYAAAAKNAIE 166
           PDNLAR-DGLRYDSASDNVFMDAEOEAKAKKANNPOHSLTKDEIKOYIKEYVOAAKNSIA 183
0YE1
                                                . :* **. : :. **:.:*
A±0YE
           -AGEDGVEIHGANGYLIDOFTODTANKRTDAWGGSVEKRARFALEVIRAVVOAVGADRTG 219
CtOYE
           -AGFDGVEIHGANGYLVDOFIODKCNORTDEYGGSVENRSKFAVEVVKAVAGAVGPEKTA 224
Lt0YE
            AGADGVEIHSANGYLLNQFLDPISNKRTDEYGGSIENRARFVLEVVDAVVDAIGEKKVG 242
           EAKADFIELHGAHGYLLDQFNQPGSNKRTDKYGGSIENRARLILEAVDACIEAVGAEHVA 295
0p0YE
Tt0YE
           -AGFDGVEIHGANGYLIDOFIODVSNORTDEYGGSVENRSRFAVEVVKAVVEAVGAERTA 225
            -AGADGVEIHSANGYLLNQFLDPHSNTRTDEYGGSIENRARFTLEVVDALVEAIGHEKVG
0YE1
            * * :*:*.*:***::** : .* *** :***:*::: :*.: *
A±0YE
           IRESPWSTFOGMRMAD----PVPOFSYLA-----RKTAESKLAYVHLVESRISGNADAE- 269
           IRLSPWSRFQGMKMDD----PRPQFLDVI----RKISGLGLAYLHLVRSGVGGPNDFNQ 275
CtOYE
           IRFSPYGTFGTMSGAS-DPGLIAQYAYVVGELEKRAKAGKRLAYIHLVEPRVTNPFFTEG
           IRLSPYAA<mark>V</mark>QGIKGVDSEIHPISYFGYVLSELERRAQEGKRLAYISVVEPRVNGIYDSKD 355
0p0YE
T+0YF
           IRLSPYGRFOGMCMKD----PVPOFEDVI-----RKINGFGLAYLHLVOTRIPGNG----
           LRLSPYGVFNSMSGGA-ETGIVAQYAYVAGELEKRAKAGKRLAFVHLVEPRVTNPFLTEG 301
A+0YF
           ----STDOLDEFLEAYGRASPYTTAGGYKADSAREAVESHYKDYDVVTGVGRPWTSNPDL 325
           AG--EDETLDFAVDLW--DGPVLIAGKLTPETARDLVDHQYKDKKVVATFGKYFISNPDL 331
CtOYE
Lt0YE
           QGWYKEGSNDFVYSIW--KGPVIRAGNYALDPR-AARDDVQKNDRTLIGYGRLFISNPDL 358
           \mathsf{KREFN}\text{---}\mathsf{TSWISEIW}\text{--}\mathsf{KGVLLRS} \textbf{G} \textbf{AY} \mathsf{LNENYKFLQHDVDENDRTLIGV} \textbf{S} \mathsf{RYYTSNPDL}
0p0YE
TtOYE
           -E--NDESLDFALRSW--DGPVLIAGGLTRESAMYLVDKEFKDKDVVATFGRYFISTPDL 327
           EGEYEGGSNDFVYSIW--KGPVIRAGNFALHPE-VVREEV-KDKRTLIGYGRFFISNPDL
0YE1
                          : .:::*
                                         .
                                                 . :: .:
A±0YE
           PEKEKAGIPLRPYEREVEYMPKDPKGYIDYEFSEEFKATLVA----- 367
           PFRIKEGIPLNPYDRSTFYTPKSPVGYTDQPFSKEFQESQTSTL----- 375
CtOYE
Lt0YE
           VORLKEGLPLNKYDRDTFYAM-TDKGYVDYPTYAEATKVAASO----- 400
           ADRLKNGHELTPYDRSKFYKHSSNDGYLTWTRYGEKEPQYKDLVDVAPEPLA 462
0p0YE
T±0YE
           PFRLKEGIELNOYDRDTFYTPKSPVGYIDOPFSKEFEALHGVQALN----- 373
           VDRLEKGLPLNKYDRDTFYOM-SAHGYIDYPTYEEALKLGWDKK------ 400
```

Figure 3. Sequence alignment of AtOYE, CtOYE, LtOYE, OpOYE, TtOYE, and OYE1. Two regions are highlighted (yellow and gray shade), representing the patterns indicative for monomeric ERs, active site residues are in blue, and FMN-binding residues are in green letters. The letters in red were used to highlight amino acids different from OYE1. The symbol (*) denotes full conservation (identical residues across all sequences), (:) indicates strong conservation (similar residues with high chemical similarity), and (.) represents weak conservation (similar residues with low chemical similarity).

Catalysts **2024**, 14, 764 5 of 16

For OYE1, several crystal structures are available, and its catalytic mechanism has been established. This makes it possible to identify at the sequence level the most important active site residues. The active site of OYE1 is composed of the following residues [29,30]: ${\rm His^{191}}$, ${\rm Asn^{194}}$, ${\rm Tyr^{196}}$, ${\rm Phe^{250}}$, and ${\rm Tyr^{375}}$ (Figure 3, blue letters). From the sequence alignment with the five fungal ERs, it becomes clear that these residues are well conserved. Only for OpOYE, the phenylalanine active site residue is different, with a valine present at that position. This may translate in a slightly larger substrate binding pocket.

OYE-type ERs typically contain a tightly bound FMN as a flavin cofactor. Nizam et al. [31] analyzed the crystal structure of OYE1 concerning the crucial residue for FMN binding. This resulted in the identification of a large set of residues interacting with the cofactor, comprising Pro^{35} , Thr^{37} , Gly^{72} , Gln^{114} , Arg^{243} , Gly^{324} , Asn^{325} , Phe^{326} , Gly^{345} , Gly^{347} , and Arg^{348} (Figure 3, green letters). The studied fungal OYEs differed in 2–3 residues out of the 11 FMN-binding residues. The observed changes concerned rather conservative mutations, suggesting that the selected proteins are capable of binding FMN.

AlphaFold2 (v2.3.1., DeepMind, London, UK) was used to predict the structures of the fungal ERs. As expected from the sequence similarity with OYE1, the predicted structures are quite similar when compared with the prototype ER (Figure 4). OYEs form a $(\beta/\alpha)8$ barrel, also known as the TIM barrel. This barrel is closed at the N-terminal edge by a short β -harpin lid [11,28]. All predicted structures displayed such architecture. The FMN is positioned inside the barrel and near the C-terminus of the β -sheet. The loops that connect the central β -strands with the α -helices were named β 1– β 8, according to the respective β -strand [28]. These regions define the oligomeric structure of the enzyme and determine the shape of the substrates and cofactor binding site. The predicted structures were compatible with binding FMN as a cofactor, as they exhibit a large cofactor binding pocket. Yet, the exact binding of the cofactor and substrates could not be predicted.

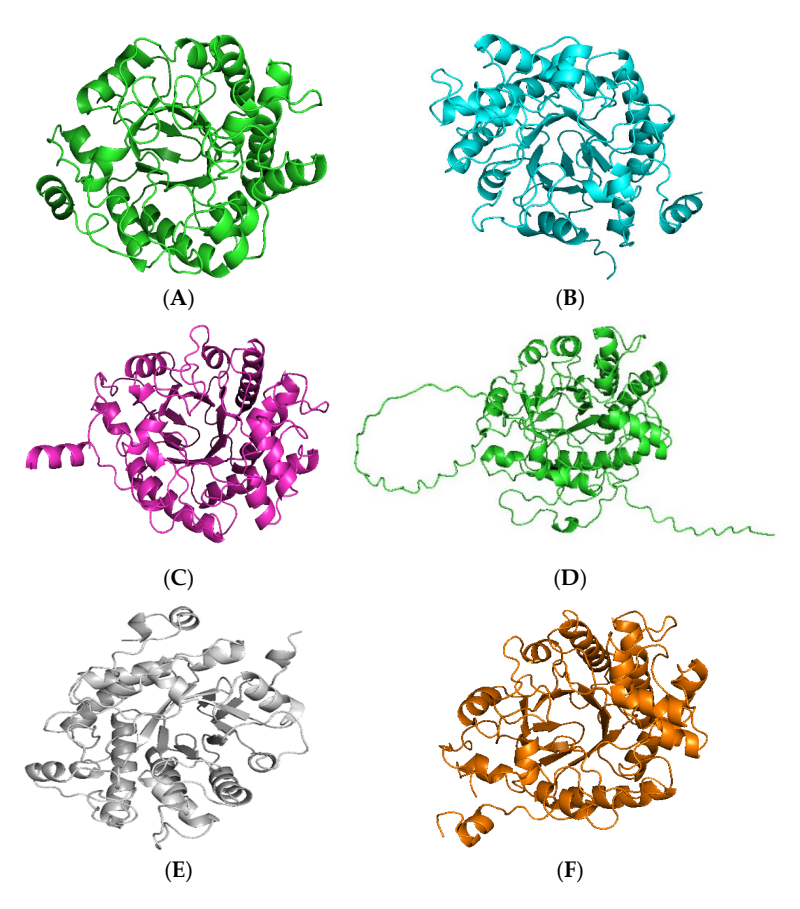


Figure 4. Structures for AtOYE (**A**), CtOYE (**B**), LtOYE (**C**), OpOYE (**D**), TtOYE (**E**), and OYE1 (**F**), as predicted by AlphaFold2 (v2.3.1, DeepMind, London, UK). The figures were generated using Pymol (v2.5.2, Schrödinger, Inc., New York, NY, USA).

Catalysts **2024**, 14, 764 6 of 16

2.2. Production and Purification of Fungal ERs

All selected proteins were expressed in *E. coli* fused to a His-tagged PTDH at their N-terminus. First, protein expression was tested on a small scale at three different temperatures, 24, 30, and 37 °C. An SDS-PAGE analysis of cell extracts revealed that all proteins could be expressed at all tested temperatures. The highest expression levels were observed at 24 °C (Figure S1—Supplementary Materials).

Next, the enzymes were expressed on a larger scale (200 mL TB medium) at 24 $^{\circ}$ C. The enzymes were purified by affinity chromatography as soluble and yellow-colored proteins. Successful purification was verified by SDS-PAGE analysis. For analyzing the gel, the calculated molecular weights for the fusion enzymes were used, which were 80.3 kDa for AtOYE, 80.9 kDa for CtOYE, 84.8 kDa for LtOYE, 91.1 kDa for OpOYE, and 80.9 for TtOYE. The proteins observed upon SDS-PAGE were in accordance with these values (Figure S2—Supplementary Materials). Their yellow appearance after purification also confirmed that they were capable of binding their flavin cofactor in a tight manner. The purified enzymes were kept in 50 mM of Tris-HCl (pH 7.5) and stored at -70 $^{\circ}$ C.

The UV-Vis absorbance spectra for all five purified enzymes were obtained (Figure 5), all displaying typical features of a flavin cofactor (two absorbance maxima at around 380 and 460 nm). Each OYE showed slightly different absorbance maxima (Table 1), reflecting variations in the protein microenvironment surrounding the isoalloxazine moiety of the FMN cofactor. By denaturation and comparison with the known extinction coefficient of FMN at 446 nm, the individual extinction coefficients of all five OYEs were determined (Table 1). This allows for an accurate quantification of FMN-bound ER, enabling accurate (kinetic) analyses. It also allowed for the quantification of the amount of purified enzyme per liter of culture. Gratifyingly, the yields obtained for all enzymes were higher than 100 mg L^{-1} . The highest yield was observed for CtOYE at 166 mg L^{-1} .

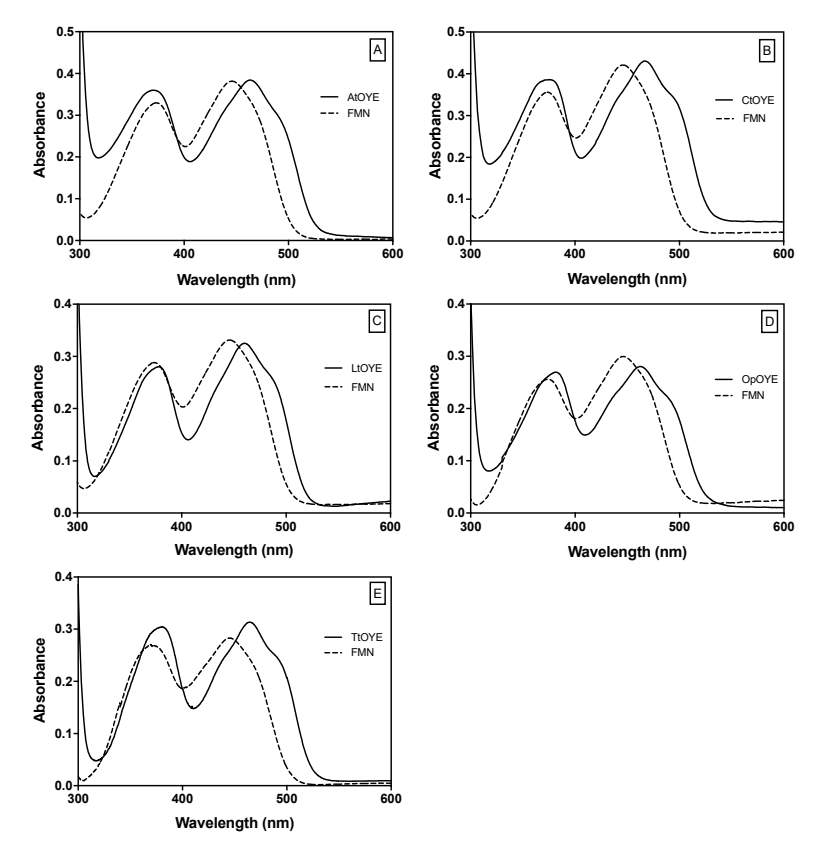


Figure 5. Absorbance spectra obtained for AtOYE (**A**), CtOYE (**B**), LtOYE (**C**), OpOYE (**D**), and TtOYE (**E**). The continued line (–) represents the spectra of the native enzymes, and the spectra with the dashed line (–-) were obtained upon unfolding.

Catalysts **2024**, 14, 764 7 of 16

Table 1. Extinction	coefficients and	vields of	purified proteins.
Table 1. Exhilicitori	coefficients and	vicius oi	purmed proteins.

Enzyme	Absorbance Maxima (nm)	Extinction Coefficient $(mM^{-1} cm^{-1})$	Yield (mg L ^{−1})
AtOYE	370, 463	13.4	147
CtOYE	376, 466	11.9	166
LtOYE	378, 459	13.0	136
OpOYE	381, 462	11.6	136
TtOYE	379, 465	12.9	117

2.3. Substrate Acceptance

To investigate the substrate specificity of the putative OYEs, various potential substrates were tested by monitoring NADPH consumption. Substrates with different electron-withdrawing groups (EWGs), such as ketones and carboxylic acids, were chosen to assess the enzymes' activity. Additionally, to explore different substrate orientations, we selected compounds where the EWG is either directly attached to an aromatic ring or positioned further from the ring with the double bond located outside the aromatic system. For all purified ERs, activity on several test substrates could be confirmed (Table 2). For checking the preference of each enzyme concerning the electron donor, activities were measured using NADPH and NADH. The activity of each enzyme with oxygen as the electron acceptor was also measured and subtracted from the activity measured for each substrate. All OYEs displayed minor but significant oxygen reactivities (Table 2).

Table 2. Specific activity (U mg^{-1}) for each enzyme using NADPH or NADH as a cofactor.

Enzyme	AtOYE (U mg ⁻¹)	CtOYE (U mg ⁻¹)	LtOYE (U mg ⁻¹)	OpOYE (U mg ⁻¹)	TtOYE (U mg ⁻¹)
Cofactor	NADPH/ NADH	NADPH/ NADH	NADPH/ NADH	NADPH/ NADH	NADPH/ NADH
O ₂	$0.2 \pm 0.1/$ 2.1 ± 0.8	$0.2 \pm 0.0 / \\ 1.1 \pm 0.2$	$0.3 \pm 0.0 / \\ 0.5 \pm 0.0$	$0.3 \pm 0.0 / \\ 0.3 \pm 0.0$	$1.0 \pm 0.1/$ 1.1 ± 0.9
	12.1 ± 1.0	1.0 ± 0.8	1.7 ± 0.4	1.9 ± 0.3	1.1 ± 0.1
1	$14.0 \pm 2.0 / \\ 6.7 \pm 3.0$	$6.3 \pm 0.1 / \\ 2.0 \pm 1.0$	$7.1 \pm 0.6 / \ 2.1 \pm 1.0$	$7.2 \pm 1.0 / \ 3.1 \pm 0.3$	$25.0 \pm 2.0 / \\ 11.7 \pm 1.0$
2 0 3	8.0 ± 0.2	n.d.	3.0 ± 0.0	0.9 ± 0.0	n.d.
4	0.5 ± 0.0	0.1 ± 0.0	0.3 ± 0.0	0.1 ± 0.0	7.3 ± 0.5
0 N O H	12.0 ± 1.0	0.8 ± 0.0	3.1 ± 0.2	2.3 ± 0.1	12.0 ± 1.0
6	0.4 ± 0.1	n.d.	0.1 ± 0.0	0.3 ± 0.1	1.7 ± 0.3

Catalysts **2024**, 14, 764 8 of 16

	_	1 1		_			
- 1	3	h	lΔ	2.	()	$\alpha \nu$	1+

Enzyme	AtOYE (U mg ⁻¹)	CtOYE (U mg ⁻¹)	LtOYE (U mg ⁻¹)	OpOYE (U mg ⁻¹)	TtOYE (U mg ⁻¹)
о он 7	0.3 ± 0.0	n.d.	n.d.	0.1 ± 0.0	0.3 ± 0.3
8	1.5 ± 0.2	n.d.	0.2 ± 0.0	0.4 ± 0.1	2.9 ± 0.5

n.d. = not detected.

For all enzymes, maleimide (5) and p-benzoquinone (2) were found to exhibit the highest activity among all the tested substrates. Specifically, AtOYE exhibited the highest specific activity for compound 5 ($12.3 \pm 1.2 \text{ U mg}^{-1}$), whereas TtOYE exhibited the highest specific activity ($25.1 \pm 2.3 \text{ U mg}^{-1}$) when acting on substrate 2. Results in Table 2 also reveal that CtOYE only shows high activity on p-benzoquinone, while it is poor or not active with the other test compounds. AtOYE, on other hand, showed activity for all substrates, showing a relaxed substrate acceptance profile. The observation that all ERs are active with benzylidenemalononitrile (1) shows that they act on enones.

A comparison of the specific activities measured for substrate 2 and cyclohex-2-en-1-one (3) revealed that all OYE activity for compound 3 was either relatively low or not detected. It reflects the reactivities of these two compounds, where p-benzoquinone is more easily reduced. This observation is also applicable for R-carvone (4), which contains only one carbonyl group near the α,β double bond and for which specific activity was generally lower for most of the enzymes.

Concerning cofactor preference, as already observed in other OYE1-type ERs, all fungal ERs prefer NADPH as a cofactor. Thus, for all subsequent analyses, NADPH was employed as the cofactor of choice.

The pH optimum of each fungal ER was determined by measuring activities at pH values ranging from pH 4 to pH 9, using maleimide as a substrate. It was found that the ERs display rather broad pH optima with maximal activities at pH 6 and 7 (Figure 6). Such pH optima for activity are common for OYE-type ERs [31,32].

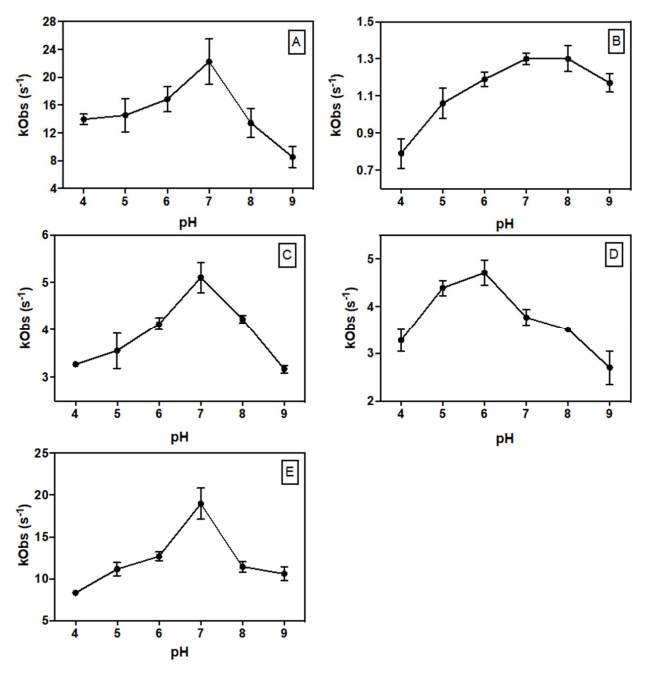


Figure 6. pH optima for AtOYE (A), CtOYE (B), LtOYE (C), OpOYE (D), and TtOYE (E).

Catalysts **2024**, 14, 764 9 of 16

2.4. Steady-State Kinetic Parameters

Considering that the enzymes showed relatively high activity toward maleimide and *p*-benzoquinone, the steady-state kinetic parameters for these two substrates and NADPH for all fungal OYEs were determined. The prototype OYE, OYE1, was also included in this kinetic analysis using maleimide as a substrate in order to be able to make a fair comparison. All obtained kinetic parameters are shown in Table 3 (for analysis of the data, see Figures S3–S5—Supplementary Materials).

Table 3. Kinetic parameters (K_M and k_{cat}) of the fungal ERs using maleimide, p-benzoquinone, and NADPH as substrates.

Enzyme	Substrate	K_M (mM)	k_{cat} (s ⁻¹)	k_{cat}/K_M (m $\mathrm{M}^{-1}\mathrm{s}^{-1}$)
	maleimide (5)	0.011 ± 0.003	25.0 ± 2.0	2340
AtOYE	<i>p</i> -benzoquinone (2)	0.9 ± 0.2	33.0 ± 1.0	36
	NADPH	0.043 ± 0.005	23.2 ± 0.8	540
	maleimide (5)	0.004 ± 0.001	1.5 ± 0.1	380
CtOYE	<i>p</i> -benzoquinone (2)	1.4 ± 0.2	18.9 ± 0.9	13
	NADPH	0.046 ± 0.002	2.7 ± 0.1	59
	maleimide (5)	0.004 ± 0.001	5.3 ± 0.1	1300
LtOYE	<i>p</i> -benzoquinone (2)	2.0 ± 0.3	25.0 ± 2.0	13
	NADPH	0.012 ± 0.002	5.2 ± 0.3	430
	maleimide (5)	0.007 ± 0.001	4.1 ± 0.1	590
OpOYE	<i>p</i> -benzoquinone (2)	1.0 ± 0.1	23.0 ± 0.8	23
	NADPH	0.011 ± 0.001	4.5 ± 0.1	400
	maleimide (5)	0.005 ± 0.001	16.3 ± 0.8	3300
TtOYE	<i>p</i> -benzoquinone (2)	1.6 ± 0.2	96.7 ± 4.0	60
	NADPH	0.012 ± 0.002	25.6 ± 1.0	2100
	maleimide (5)	0.003 ± 0.001	4.4 ± 0.1	1500
OYE1	<i>p</i> -benzoquinone (2)	-	=	-
	NADPH	0.013 ± 0.003	4.8 ± 0.3	370

In relation to maleimide, all the enzymes presented similar affinity for the substrate. AtOYE and TtOYE appeared to be more catalytically efficient. As expected, LtOYE presented similar values of k_{cat} and K_M in comparison to its homologue, OYE1. Maleimide is a common substrate used for ene-reductases, and various catalytic efficiencies have been reported for this compound ranging from 10,800 mM⁻¹s⁻¹ [31] to 300 mM⁻¹s⁻¹ [33]. The newly identified ERs exhibited catalytic efficiencies of 380–3300 mM⁻¹s⁻¹ (Table 3).

For p-benzoquinone, the studied enzymes exhibited K_M values within the range of 1–2 mM. The $k_{\rm cat}$ values ranged from 1.3 to 27.7 s⁻¹. Compared with maleimide, the K_M values were 2–3 orders of magnitude lower, indicating that maleimide was preferred by the enzymes. Similarly, as observed for maleimide, TtOYE presented the highest k_{cat}/K_M ratio for p-benzoquinone among the enzymes investigated, indicating a particularly high catalytic efficiency.

Using maleimide at a fixed concentration, the kinetic parameters for NADPH were determined (Table 3, Figure S3). All the enzymes showed high affinity for NADPH, with the highest k_{cat}/K_M ratio observed for TtOYE again.

2.5. Bioconversion

The reduction of *R*-carvone is of significant interest, primarily due to the versatility of its product, dihydrocarvone, which finds applications in various fields. Ene-reductases offers the advantage of achieving asymmetric reduction and producing a single product. The level of conversion and *d.e.* were determined for all fungal ERs. The chromatograms and mass spectra are available in the Supplementary Materials (Figure S6). All enzymes suc-

Catalysts 2024, 14, 764 10 of 16

cessfully converted the substrate into the desired product (Table 4). Both AtOYE and TtOYE achieved nearly complete conversion. In contrast, OpOYE exhibited a conversion rate of less than 50%. OpOYE exhibited poor stereoselectivity, yielding (R,R)-dihydrocarvone as the major product, while also producing the second diastereomer (S,R), resulting in a diastereomeric excess (d.e.) of 92%. The other ERs consistently achieved a d.e. exceeding 99%.

Table 4.	Conversion of	of R-carvone	by fungal ERs.
----------	---------------	--------------	----------------

Enzyme	Conversion (%)	d.e. (%)/(config.)
AtOYE	99	>99/ <i>R</i> , <i>R</i>
CtOYE	73	>99/ <i>R</i> , <i>R</i>
LtOYE	70	>99/ <i>R</i> , <i>R</i>
OpOYE	43	92/R,R
TŧOYE	91	>99/ <i>R</i> , <i>R</i>

config.—absolute configuration.

These results align with the literature, where R-carvone is commonly used to test the stereospecificity of ene-reductases, typically yielding (R,R)-dihydrocarvone with high d.e. values [34,35]. It is important to note that the configuration was established by comparison with the chromatogram of commercial dihydrocarvone, which shows a higher concentration of the R,R stereoisomer (Figure S7—Supplementary Materials).

2.6. Thermostability

The studied ERs originate from fungi that thrive at relatively high temperatures. Therefore, it was anticipated that these enzymes exhibit higher thermostabilities when compared with other known ERs, such as OYE1. Apparent melting temperatures (T_m) were determined for all fungal ERs and OYE1. The thermostability of OYE1 was found to be identical to LtOYE, with T_m values of 48.8 °C. All other ERs were found to be significantly more thermostable, with OpOYE and CtOYE being the most thermostable (T_m values of 61.5 and 62.5 °C, respectively). The other two ERs displayed intermediate thermostabilities, with a T_m value of 53.5 °C for AtOYE and 57.5 °C for TtOYE. Robescu et al. [19] isolated four ERs from fungi, of which two, AnOYE8 and BfOYE4, belonged to the thermophilic-like Class III ERs. Still, these fungal ERs displayed T_m values of merely 43–44 °C. Clearly, the fungal ERs identified in this study represent more robust variants.

After establishing the thermostability of these newly identified enzymes, the impact of solvents on thermostability was studied. The melting temperature of each OYE was measured in the presence of three commonly used solvents, namely DMSO, ethanol, and methanol. A range of solvent concentrations (5–50% v/v) was tested for each solvent and ER. Solvent tolerance is an important feature when considering enzymes for biocatalysis, which often involves the use of solvents. As expected, for every OYE and solvent combination, increasing the solvent concentration resulted in lowered thermostability (Figure 7). Ethanol had the most drastic effect on thermostability. For DMSO and methanol, the curves presented a similar behavior when varying the solvent concentration between 5 and 20% v/v. Beyond this concentration range, a more drastic loss in the thermostability was observed for methanol. DMSO seems to be the mildest solvent when considering the effect on thermostability. ERs from thermophilic bacteria [20,36] were found to be the most tolerant toward DMSO, analogous to the findings observed within the present study.

Another study conducted in relation to thermostability was to check the influence of pH on melting temperatures. As illustrated by the curves in Figure 8, the thermostabilities of the fungal ERs were minimally affected between pH values 5 and 9. Only at pH 4 did the thermostability decrease significantly. OYE1 displayed a somewhat different behavior, with a relatively sharp decline at higher pH values, highlighting the difference between the studied fungal ERs and OYE1.

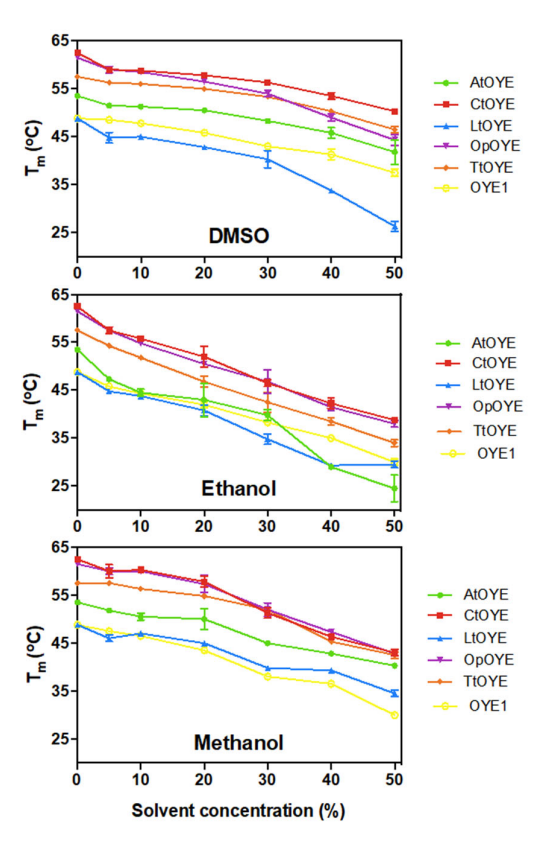


Figure 7. Effect of solvents on melting temperatures of ERs.

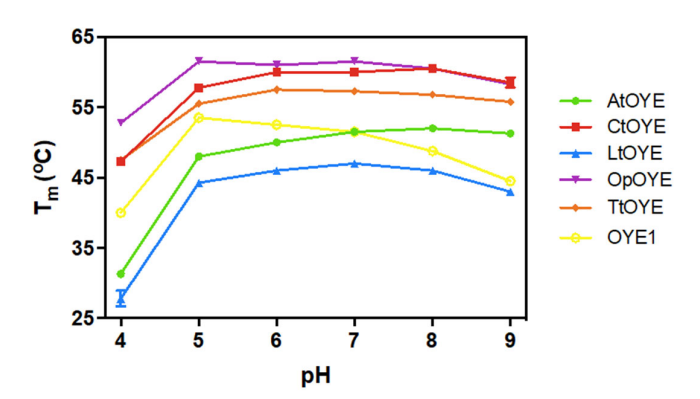


Figure 8. Melting temperatures (T_m) measured for ERs at different pH values.

3. Materials and Methods

3.1. Chemicals, Strains, and Enzymes

T4 ligase and the restriction enzyme BsaI were purchased from *New England Biolabs*. *E. coli* NEB 10-β (*NEB*, Ipswich, MA, USA) strains were used as the host for cloning and protein expression. Mesitylene (98%), benzylidenemalononitrile (98%), *R*-carvone (98%), dihydrocarvone (98%—mixture of isomers), cinnamic acid (97%), cyclohex-2-en-1-one (98%), maleimide (99%), methyl cinnamate (99%), *p*-benzoquinone (98%), trans-4-phenyl-but-3-en-2-one (99%), and dimethyl sulfoxide (DMSO) were obtained from Sigma-Aldrich (St. Louis, MO, USA). Purified OYE1 was a kind gift from Dr. Y. Tong (University of Groningen).

3.2. Bioinformatic Analysis

The genes corresponding to the studied ERs were obtained through the National Center for Biotechnology Information—NCBI. BLASTp (protein–protein Basic Local Alignment Search Tool) was used, using the OYE1 gene sequence as a query. The search re-

Catalysts 2024, 14, 764 12 of 16

sulted in five predicted proteins from the following fungi: *A. thermomutatus* (NCBI code: XP_026612299.1), *C. thermophilium* (NCBI code: XP_006694066.1), *L. thermotolerans* (NCBI code: XP_002553824.1), *O. polymorpha* (NCBI code: KAH3658896.1), and *T. terrestris* (NCBI code: XP_003652740.1). The phylogenetic tree was constructed using the software MEGA v.11 [37] using the maximum likelihood method based on the JTT matrix-based model [38] and using sequences from ERs previously identified [9] (the accession number of each ER is in the Supplementary Materials—Table S1). The tree was constructed after all ER sequences were aligned using Clustal-Omega (EMBL-EBI/Hinxton).

3.3. Plasmid Construction

Synthetic DNA fragments were obtained (Twist Bioscience, San Francisco, CA, USA), encoded for each enzyme and optimized for expression in *E. coli*. The fragments were cloned into the pCRE vector [39] using the Golden Gate method [40]. The vector was chosen because it allows for the expression of recombinant proteins with an N-terminal His6x-tag and PTDH as an additional fusion protein. The sequence of six histidine enables purification by affinity chromatography. The presence of PTDH as a fusion protein between the N-terminal His-tag and the ER facilitates the regeneration of the reduced nicotinamide cofactor required by the ERs using phosphite as sacrificial cosubstrate. PTDH as a fusion partner was also found to have a positive effect on the expression of soluble protein [39]. To verify correct cloning, the plasmids were isolated and sent for sequencing (Eurofins, Hamburg, BL, Germany).

3.4. Expression

Competent *E. coli* cells were transformed with the expression plasmids for each protein and grown on LB (lysogenic broth) plates containing 50 μg mL⁻¹ ampicillin. Single colonies were transferred into a test tube with 5 mL LB medium and 50 μg mL⁻¹ ampicillin and subsequently grown overnight to be used as a pre-culture. Next, cells from the pre-culture were transferred to 30 mL of TB (terrific broth) medium containing 50 μ g mL⁻¹ ampicillin and incubated at 37 °C while shaking at 135 rpm. Protein expression was induced by the addition of L-arabinose (0.02% v/v) when the OD₆₀₀ reached 0.6–0.8. Then, cells were grown at 24, 30, and 37 °C for another 14–16 h while shaking at 135 rpm. After this period, cells were harvested by centrifugation ($4420 \times g$, 20 min, 4 °C), the supernatant was discarded, and the pellet was resuspended in 7 mL lysis buffer (50 mM Tris-HCl pH 7.5, 150 mM NaCl, $1 \mu g mL^{-1}$ DNAse, 0.1 mM phenylmethylsulphonyl fluoride). Cells were disrupted by ultrasonic treatment (3" on and 3" off for 5 min, 70% amplitude) and the extract obtained was cleared by centrifugation (11,000 rpm, 40 min, 4 °C). The determination of the best temperature for expression was evaluated by SDS-PAGE analysis. After determining the optimal expression temperature, expression was scaled up. For this, 5 mL of pre-culture was transferred into 200 mL TB medium for growing cells. The cells, after induction, growth, and centrifugation, were resuspended in 15 mL of lysis buffer and ultrasonication was carried out for 10 min (5" on and 7" off, 70% amplitude). A cleared cell extract was obtained by centrifugation.

3.5. Purification

Since the expressed proteins contained a His-tag, the purification was performed using 3 mL HisTrap Ni-Sepharose HP columns (GE Healthcare Lifesciences, Boston, MS USA). The column was first equilibrated with 50 mM Tris-HCl, 100 mM NaCl, and pH 7.5. The cleared cell extract was loaded on the column after using a microfilter (\emptyset = 0.2 μ m) in order to remove small precipitates. To increase the interaction between the proteins and the nickel, the column material was gently mixed for 1 h at 4 °C. Then, the column was washed with 50 mM Tris-HCl (pH 7.5) containing 5 mM imidazole. After washing, the protein was eluted with 50 mM Tris-HCl and 500 mM imidazole (pH = 7.5). The collected volume of the yellow-colored enzyme fraction was 2.5 mL. The enzyme sample was subsequently desalted using a PD10 desalting column (Cytiva-Global Life Sciences Solutions, Morrisville, NC,

USA) using 50 mM Tris-HCl (pH 7.5). The purified proteins were analyzed by SDS-PAGE. Aliquots of purified proteins were frozen using liquid nitrogen and stored at -70 °C until further use.

3.6. Spectral Analysis

Absorbance spectra were obtained by a UV spectrophotometer (Jasco V-660/650/730, Tokyo, Japan) measuring absorbance from 300 to 600 nm at 25 °C. After collecting a spectrum of native protein, the protein was denatured by heating the sample at 95 °C for 20 min. The absorbance spectrum of the denatured protein sample was subsequently collected and used to determine the extinction coefficient of each flavoprotein based on the extinction coefficient of FMN ($\varepsilon_{446} = 12.2 \text{ mM cm}^{-1}$).

3.7. Enzyme Analysis

Enzyme activity was measured by monitoring the consumption of NADH or NADPH at 340 or 365 nm using a spectrophotometer. Assays were performed in 100 μ L of 50 mM Tris-HCl (pH 7.5) containing 1.0 mM of the test substrate and 10–50 nM enzyme (TtOYE—10 nM; AtOYE—20 nM; CtOYE, LtOYE, and OpOYE—50 nM) at 25 °C. The activity was expressed in units where 1 unit (U) is defined as the amount of enzyme necessary to convert 1 μ M mol NAD(P)H in 1 min. The following compounds were tested as substrates: benzylidenemalononitrile, *R*-carvone, cinnamic acid, cyclohex-2-en-1-one maleimide, methyl cinnamate, *p*-benzoquinone, and trans-4-phenyl-but-3-en-2-one. The ability of the reductases to use dioxygen as electron acceptor, essentially acting as a NAD(P)H oxidase, was also investigated. When such NAD(P)H consumption activity was observed in absence of an ene substrate, the reported ene reduction activity was corrected for this futile reactivity. Activity screening was performed with both nicotinamide cofactors, NADH and NADPH, to establish cofactor preference.

For a more detailed kinetic analysis, two substrates, maleimide and p-benzoquinone, were selected and used to determine the steady-state kinetic parameters, K_M and k_{cat} . For this, the consumption of NADPH was monitored at 340 nm in 100 μ L of 50 mM Tris-HCl (pH 7.5) containing 100 μ M NADPH, 10–50 nM enzyme (TtOYE—10 nM; AtOYE—20 nM; CtOYE, LtOYE, and OpOYE—50 nM), and 1.0 mM maleimide or p-benzoquinone. The procedure was repeated to calculate the K_M and k_{cat} for NADPH for each enzyme. For this, the nicotinamide concentration ranged between 5 and 200 μ M and maleimide was used at a fixed concentration (1.0 mM). The data were fitted using the Michaelis—Menten equation in the program GraphPad Prism v. 6.07 (GraphPad Software, San Diego, CA, USA).

The pH optima for activity were determined by the using several buffers, which were 50 mM acetate buffer for pH 4.0 and 5.0, 50 mM KP $_{\rm i}$ buffer for pH 6.0 and 7.0, and 50 mM Tris-HCl buffer for pH 8.0 and 9.0. For each buffer, the consumption of NADPH (0.10 mM) was monitored at 340 nm using maleimide (1.0 mM) as a substrate. All the measurements were performed in triplicate.

3.8. Bioconversions

The bioreduction of R-carvone (4) by the ERs was carried out in 100 mM Tris-HCl (pH 7.5) containing 10 mM substrate (dissolved in 1% v/v DMSO), 0.20 mM NADPH, 30 nM of the respective purified enzyme, and 20 mM of sodium phosphite. The reaction mixture (final volume = 1 mL) was incubated at 25 °C for 12 h under agitation (400 rpm). They were terminated by adding ethyl acetate (1:1, v/v), enabling product extraction. The sample was then subjected to centrifugation, separating the organic phase from the aqueous phase. Ethyl acetate was added to the aqueous phase once more (1:1, v/v) to ensure thorough extraction. The resulting second organic phase was combined with the first, and the combined solution was dehydrated using Na₂SO₄. Mesitylene (0.02% v/v) was added to the ethyl acetate before extraction to serve as an internal standard.

The conversion and *d.e.* were determined by GC-MS using an HP-5MS column (30 m \times 0.25 mm \times 0.25 μ m, Agilent, Santa Clara, CA, USA). A 1 μ L sample was injected

Catalysts 2024, 14, 764 14 of 16

with helium as the carrier gas (flow rate: 1.7 mL/min) using a 10:1 split ratio, and injection was performed at 300 °C. The temperature program included a ramp of 20 °C/min from 40 °C to 325 °C, followed by a 5 min hold at 325 °C. The mass spectrometer operated as the detector, utilizing electron ionization (EI) at 70 eV and maintaining an ion source temperature of 200 °C. Fragment ions were detected within the 35–500 Da range. Retention times were 6.9 min for mesitylene (internal standard), 11.9 min for *R*-carvone, 11.2 min for 2R,5R-dihydrocarvone, and 11.3 min for (2S,5R)-dihydrocarvone.

The chromatogram for commercial dyhidrocarvone was obtained by GC-MS (Shimadzu GC2010 Plus, MS2010 Plus, Hercule, CA, USA) in electron ionization mode (70 eV). A 1.0 μ L sample was injected into a DB5 column (30 m \times 0.25 mm \times 0.25 μ m) with injector and interface temperatures of 250 °C and 270 °C. The oven temperature was held at 90 °C for 4 min, then ramped to 280 °C at 10 °C/min (held for 5 min), followed by an increase to 300 °C (held for 10 min). The total analysis time was 40 min. Helium (0.75 mL/min) was used as a carrier gas with a split ratio of 20:1. Fragment ions were detected between 40 and 550 Da.

3.9. Analysis of Thermostability

Unfolding temperatures (T_m) for all enzymes were determined in various conditions as follows: in 50 mM Tris-HCl, pH 7.5; in the presence of cosolvents (ethanol, DMSO, and methanol) at different concentrations (5–50% v/v); and at different pH values by using three different buffers (50 mM acetate buffer for pH 4.0 and 5.0, 50 mM KP_i buffer for pH 6.0 and 7.0, and 50 mM Tris-HCl buffer for pH 8.0 and 9.0). For assessing thermostability, the ThermoFAD procedure was utilized, which depends on the fluorescence of the bound flavin cofactor [41]. Samples of 20 μ L were used, containing 10 μ M enzyme. The measurements were carried out in an RT–PCR machine (CFX96–Bio-Rad, Hercule, CA, USA) using an excitation filter setting of 450–490 nm and emission filter setting of 515–530 nm. The fluorescence was monitored while ramping the temperature from 25 °C until 90 °C at 0.5 °C per 30 s. Each reported T_m is based on two measurements.

4. Conclusions

The five selected fungal ERs could be well expressed as soluble and functional flavoenzymes in a bacterial expression host. Characterization of the ERs revealed that they indeed function as OYE-type ERs. They all prefer NADPH as an electron donor and each OYE was shown to be efficient in reducing one or more of the tested compounds. Except for one fungal ER, LtOYE, all other studied ERs displayed much higher thermostabilities when compared with the prototype ER, OYE1. CtOYE and OpOYE were shown to be the most stable, with melting temperatures of $>60~^{\circ}$ C. This again confirms that mining enzymes from thermophilic organisms is efficient in expanding the toolbox of available robust biocatalysts.

Substrate screening revealed that AtOYE exhibits a rather broad substrate scope, being active on all tested compounds. TtOYE showed relatively high catalytic efficiencies. Using *R*-carvone, both enzymes, AtOYE and TtOYE, promoted almost the complete conversion into the product desired. The data show that with this newly identified set of OYEs, new robust biocatalysts have been identified with attractive biocatalytic properties.

Supplementary Materials: The following supporting information can be downloaded at: https://www.mdpi.com/article/10.3390/catal14110764/s1, Figure S1: SDS-PAGE analysis for expression on small scale; Figure S2: SDS-PAGE analysis of purified enzymes; Figure S3: Michaelis–Menten curves obtained by the software GraphPad Prism for measurement of kinetic parameters (K_M and k_{cat}) for the enzymes AtOYE, CtOYE, LtOYE, OpOYE, TtOYE, and OYE1 using maleimide as substrate; Figure S4: Michaelis–Menten curves obtained by the software GraphPad Prism for measurement of kinetic parameters (K_M and k_{cat}) for the enzymes AtOYE, CtOYE, LtOYE, OpOYE, and TtOYE using p-benzoquinone as a substrate; Figure S5: Michaelis–Menten curves were generated using GraphPad Prism software to determine the kinetic parameters (K_M and K_{cat}) of the enzymes AtOYE, CtOYE, LtOYE, OpOYE, TtOYE, and OYE1 for NADPH; Figure S6: Chromatograms and mass spectra ob-

Catalysts 2024, 14, 764 15 of 16

tained during the bioconversion of R-carvone; Figure S7: Chromatogram illustrating the composition of commercial dihydrocarvone. Table S1: List of putative and obtained ene-reductases described in the literature, with the enzymes' source (bacteria, fungi, algae, and plants) and the NCBI access code; Table S2: Unfolding temperatures (T_m) measured by the ThermoFAD procedure in the presence of different solvents; Table S3: Unfolding temperatures (T_m) measured by the ThermoFAD procedure in different pHs.

Author Contributions: P.H.D.: investigation, formal analysis, data curation, writing—original draft preparation; M.W.F.: conceptualization, supervision, resources, writing—review and editing. All authors have read and agreed to the published version of the manuscript.

Funding: P. H. Damada thanks the University of Groningen and Coordenação de Aperfeiçoamento de Pessoal de Nível Superior-Brazil (CAPES-88887.372100/2019-00) for the financial support.

Data Availability Statement: The data presented in this study are available upon request from the corresponding author.

Acknowledgments: We thank Yapei Tong for providing purified OYE1.

Conflicts of Interest: The authors declare no conflicts of interest.

References

 Gatti, F.G.; Parmeggiani, F.; Sacchetti, A. Synthetic strategies based on C=C bioreductions for the preparation of biologically active molecules. In Synthetic Methods for Biologically Active Molecules, 1st ed.; Brenna, E., Ed.; Wiley: Hoboken, NJ, USA, 2013; pp. 49–84.

- 2. Toogood, H.S.; Scrutton, N.S. Discovery, characterization, engineering, and applications of ene-reductases for industrial biocatalysis. *ACS Catal.* **2018**, *8*, 3532–3549. [PubMed]
- 3. Hecht, K.; Buller, R. Ene-reductases in pharmaceutical chemistry. In *Pharmaceutical Biocatalysis: Chemoenzymatic Synthesis of Active Pharmaceutical Ingredients*; Grunwald, P., Ed.; Jenny Stanford: Singapore, 2019.
- 4. Mathew, S.; Trajkovic, M.; Kumar, H.; Nguyen, Q.T.; Fraaije, M.W. Enantio- and regioselective ene -reductions using F420H2-dependent enzymes. *Chem. Commun.* **2018**, *54*, 11208–11211.
- 5. Warburg, O.; Christian, W. Yellow enzyme and its effects. Biochemistry 1933, 266, 377–411.
- 6. Knaus, T.; Toogood, H.S.; Scrutton, N.S. Ene-reductases and their applications. In *Green Biocatalysis*; Patel, R.N., Ed.; John Wiley & Sons, Inc: Hoboken, NJ, USA, 2016; pp. 473–488.
- 7. Scholtissek, A.; Tischler, D.; Westphal, A.; Van Berkel, W.; Paul, C. Old yellow enzyme-catalysed asymmetric hydrogenation: Linking family roots with improved catalysis. *Catalysts* **2017**, 7, 130. [CrossRef]
- 8. Kitzing, K.; Fitzpatrick, T.B.; Wilken, C.; Sawa, J.; Bourenkov, G.P.; Macheroux, P.; Clausen, T. The 1.3 Å crystal structure of the flavoprotein YqJM reveals a novel class of old yellow enzymes. *J. Biol. Chem.* **2005**, 280, 27904–27913.
- 9. Böhmer, S.; Marx, C.; Gómez-Baraibar, Á.; Nowaczyk, M.M.; Tischler, D.; Hemschemeier, A.; Happe, T. Evolutionary diverse *Chlamydomonas reinhardtii* old yellow enzymes reveal distinctive catalytic properties and potential for whole cell biotransformation. *Algal Res.* **2020**, *50*, 101970.
- 10. Stuermer, R.; Hauer, B.; Hall, M.; Faber, K. Asymmetric bioreduction of activated C=C bonds using enoate reductases from the old yellow enzyme family. *Curr. Opin. Chem. Biol.* **2007**, *11*, 203–213.
- 11. Williams, R.E.; Bruce, N.C. 'New uses for an old enzyme'—The old yellow enzyme family of flavoenzymes. *Microbiology* **2002**, 148, 1607–1614.
- 12. Knowles, W.S.; Noyori, R. Pioneering perspectives on asymmetric hydrogenation. Acc. Chem. Res. 2007, 40, 1238–1239.
- 13. Kumar Roy, T.; Sreedharan, R.; Ghosh, P.; Gandhi, T.; Maiti, D. Ene-reductase: A multifaceted biocatalyst in organic synthesis. *Chem.—A Eur. J.* **2022**, *28*, e202103949.
- 14. Kohli, R.M.; Massey, V. The oxidative half-reaction of old yellow enzyme. J. Biol. Chem. 1998, 273, 32763–32770. [CrossRef]
- 15. Parmeggiani, F.; Brenna, E.; Colombo, D.; Gatti, F.G.; Tentori, F.; Tessaro, D. "A study in yellow": Investigations in the stereoselectivity of ene-reductases. *ChemBioChem* **2022**, 23, e202100445. [CrossRef] [PubMed]
- 16. Winkler, C.K.; Tasnádi, G.; Clay, D.; Hall, M.; Faber, K. Asymmetric bioreduction of activated alkenes to industrially relevant optically active compounds. *J. Biotechnol.* **2012**, *162*, 381–389. [CrossRef]
- 17. Atalah, J.; Cáceres-Moreno, P.; Espina, G.; Blamey, J.M. Thermophiles and the applications of their enzymes as new biocatalysts. *Bioresour. Technol.* **2019**, *280*, 478–488. [CrossRef] [PubMed]
- 18. Littlechild, J.A. Improving the 'toolbox' for robust industrial enzymes. J. Ind. Microbiol. Biotechnol. 2017, 44, 711–720. [CrossRef]
- 19. Robescu, M.S.; Loprete, G.; Gasparotto, M.; Vascon, F.; Filippini, F.; Cendron, L.; Bergantino, E. The family keeps on growing: Four novel fungal OYEs characterized. *Int. J. Mol. Sci.* **2022**, *23*, 3050. [CrossRef]
- 20. Robescu, M.S.; Niero, M.; Loprete, G.; Cendron, L.; Bergantino, E. A new thermophilic ene-reductase from the filamentous anoxygenic phototrophic bacterium *Chloroflexus aggregans*. *Microorganisms* **2021**, *9*, 953. [CrossRef]
- 21. Maheshwari, R.; Bharadwaj, G.; Bhat, M.K. Thermophilic fungi: Their physiology and enzymes. *Microbiol. Mol. Biol. Rev.* **2000**, *64*, 461–488. [CrossRef]

22. Ejmal, M.A.; Holland, D.J.; MacDiarmid, R.M.; Pearson, M.N. The effect of Aspergillus thermomutatus chrysovirus 1 on the biology of three Aspergillus species. Viruses 2018, 10, 539. [CrossRef]

- 23. Benassi, V.M.; Lucas, R.C.D.; Jorge, J.A.; Polizeli, M.d.L.T.d.M. Screening of thermotolerant and thermophilic fungi aiming β-xylosidase and arabinanase production. *Braz. J. Microbiol.* **2014**, *45*, 1459–1467. [CrossRef]
- 24. Tansey, M.R. Effect of temperature on growth rate and development of the thermophilic fungus *Chaetomium Thermophile*. *Mycologia* **1972**, *64*, 1290–1299. [CrossRef]
- 25. Velasco, J.; Oliva, B.; Gonçalves, A.L.; Lima, A.S.; Ferreira, G.; França, B.A.; Mulinari, E.J.; Gonçalves, T.A.; Squina, F.M.; Kadowaki MA, S.; et al. Functional characterization of a novel thermophilic exo-arabinanase from *Thermothielavioides terrestris*. *Appl. Microbiol. Biotechnol.* **2020**, *104*, 8309–8326. [CrossRef] [PubMed]
- 26. Morata, A.; Loira, I.; Tesfaye, W.; Bañuelos, M.; González, C.; Suárez Lepe, J. *Lachancea thermotolerans* applications in wine technology. *Fermentation* **2018**, *4*, 53. [CrossRef]
- 27. Liebal, U.W.; Fabry, B.A.; Ravikrishnan, A.; Schedel, C.V.; Schmitz, S.; Blank, L.M.; Ebert, B.E. Genome-scale model reconstruction of the methylotrophic yeast *Ogataea polymorpha*. *BMC Biotechnol*. **2021**, 21, 23. [CrossRef]
- 28. Oberdorfer, G.; Steinkellner, G.; Stueckler, C.; Faber, K.; Gruber, K. Stereopreferences of old yellow enzymes: Structure correlations and sequence patterns in enoate reductases. *ChemCatChem* **2011**, *3*, 1562–1566. [CrossRef]
- 29. Nizam, S.; Verma, S.; Borah, N.N.; Gazara, R.K.; Verma, P.K. Comprehensive genome-wide analysis reveals different classes of enigmatic old yellow enzyme in fungi. *Sci. Rep.* **2014**, *4*, 4013. [CrossRef]
- 30. Brown, B.J.; Deng, Z.; Karplus, P.A.; Massey, V. On the active site of old yellow enzyme. *J. Biol. Chem.* **1998**, 273, 32753–32762. [CrossRef]
- 31. Nizam, S.; Gazara, R.K.; Verma, S.; Singh, K.; Verma, P.K. Comparative structural modeling of six old yellow enzymes (OYEs) from the necrotrophic fungus Ascochyta rabiei: Insight into novel OYE classes with differences in cofactor binding, organization of active site residues and stereopreferences. *PLoS ONE* **2014**, *9*, e95989. [CrossRef]
- 32. Riedel, A.; Mehnert, M.; Paul, C.E.; Westphal, A.H.; Van Berkel, W.J.H.; Tischler, D. Functional characterization and stability improvement of a 'thermophilic-like' ene-reductase from *Rhodococcus opacus* 1CP. *Front. Microbiol.* **2015**, *6*, 1073. [CrossRef]
- 33. Aregger, D.; Peters, C.; Buller, R.M. Characterization of the novel ene reductase Ppo-ER1 from *Paenibacillus polymyxa*. *Catalysts* **2020**, *10*, 254. [CrossRef]
- 34. Fu, Y.; Castiglione, K.; Weuster-Botz, D. Comparative characterization of novel ene-reductases from cyanobacteria. *Biotechnol. Bioeng.* **2013**, *110*, 1293–1301. [CrossRef] [PubMed]
- 35. Ni, Y.; Yu, H.L.; Lin, G.Q.; Xu, J.H. An ene reductase from *Clavispora lusitaniae* for asymmetric reduction of activated alkenes. *Enzym. Microb. Technol.* **2014**, *56*, 40–45. [CrossRef]
- 36. Tischler, D.; Gädke, E.; Eggerichs, D.; Gomez Baraibar, A.; Mügge, C.; Scholtissek, A.; Paul, C.E. Asymmetric reduction of (*R*)-carvone through a thermostable and organic-solvent-tolerant ene-reductase. *ChemBioChem* **2020**, *21*, 1217–1225. [CrossRef] [PubMed]
- 37. Tamura, K.; Stecher, G.; Kumar, S. MEGA 11: Molecular Evolutionary Genetics Analysis Version 11. *Mol. Biol. Evol.* **2021**, *38*, 3022–3027. [CrossRef] [PubMed]
- 38. Jones, D.T.; Taylor, W.R.; Thornton, J.M. The rapid generation of mutation data matrices from protein sequences. *Comput. Appl. Biosci.* **1992**, *8*, 275–282. [CrossRef]
- 39. Torres Pazmiño, D.E.; Riebel, A.; De Lange, J.; Rudroff, F.; Mihovilovic, M.D.; Fraaije, M.W. Efficient biooxidations catalyzed by a new generation of self-sufficient Baeyer-Villiger monooxygenases. *ChemBioChem* **2009**, *10*, 2595–2598. [CrossRef]
- 40. Engler, C.; Kandzia, R.; Marillonnet, S. A one pot, one step, precision cloning method with high throughput capability. *PLoS ONE* **2008**, *3*, e3647. [CrossRef]
- 41. Forneris, F.; Orru, R.; Bonivento, D.; Chiarelli, L.R.; Mattevi, A. ThermoFAD, a ThermoFluor®-adapted flavin ad hoc detection system for protein folding and ligand binding. *FEBS J.* **2009**, *276*, 2833–2840. [CrossRef]

Disclaimer/Publisher's Note: The statements, opinions and data contained in all publications are solely those of the individual author(s) and contributor(s) and not of MDPI and/or the editor(s). MDPI and/or the editor(s) disclaim responsibility for any injury to people or property resulting from any ideas, methods, instructions or products referred to in the content.